

# Oldhamite: a new mineral in mantle for C-O-S-Ca cycles and an indicator for planetary habitability

Yuegao Liu<sup>1†</sup>, I-Ming Chou<sup>1</sup>, Jiangzhi Chen<sup>1‡</sup>, Oliver Tschauner<sup>2</sup>, Nanping Wu<sup>1</sup>, Wenyuan Li<sup>3</sup>, Leon Bagas<sup>3</sup>, Minghua Ren<sup>2</sup>, Shenghua Mei<sup>1\*</sup>, Liping Wang<sup>4\*</sup>

<sup>1</sup>CAS Key Laboratory for Experimental Study under Deep-sea Extreme Conditions, Institute of Deep-sea Science and Engineering, Chinese Academy of Sciences; No. 28 Luhuitou Road, Sanya 572000, Hainan, China.

<sup>2</sup>Department of Geoscience, University of Nevada, Las Vegas; 4505 S. Maryland Pkwy, Las Vegas, NV 89154, United States.

<sup>3</sup>Xi'an Center of China Geological Survey; No. 438 Youyi Road, Xi'an 710054, Shaanxi, China.

<sup>4</sup>Academy for Advanced Interdisciplinary Studies, Southern University of Science and Technology; No. 1088, Xueyuan Avenue, Shenzhen 518055, Guangdong, China.

\*Corresponding author. Email: mei@idsse.ac.cn (S.H.M); wanglp3@sustech.edu.cn (L.P.W)

†‡ These authors contributed equally to this work.

## Abstract

In the solar system, oldhamite (CaS) is generally considered to be formed by the condensation of solar nebula gas. Enstatite chondrites, one of the most important repositories of oldhamite, are believed to be the representative of the material which formed Earth. Thus, the formation mechanism and the evolution process of oldhamite are of great significance to the deeply understanding about the solar nebula, meteorites, the origin of Earth, and the C-O-S-Ca cycles of Earth. To date, no report about the oldhamite in the mantle exists. However, here we show the formation of oldhamite through the reaction between sulfide-bearing orthopyroxenite and molten  $\text{CaCO}_3$  at 1.5 GPa/1510 K and 0.5 GPa/1320 K. Surprisingly the oxygen fugacities in our experiments are within the range of mantle conditions, which is at least 6 orders of magnitude higher than that of the solar nebula mechanism. Oldhamite is easily

oxidized to  $\text{CaSO}_4$ . Low oxygen fugacity of magma and extreme low oxygen content of atmosphere are necessary for existence of oldhamite on the surface of a planet; otherwise, anhydrite or gypsum will exist in large quantities. The widespread existence of oldhamite on the planet's surface indicates the planet is definitely not habitable. The formation and oxidation of oldhamite are accompanied by the production of  $\text{CO}_2$  and the consumption of  $\text{O}_2$ , which may have impact on the ecosystem of planets.

## Keywords

Oldhamite, middle ocean ridge, large igneous province, crustal contamination, mantle metasomatism, planetary habitability.

## Introduction

The alkaline- and alkaline-earth sulfides such as oldhamite ( $\text{CaS}$ ) are extremely rare in terrestrial rocks. To date, only two studies report the suspected discovery of oldhamite in natural terrestrial rocks. One is in volcanic glass from the Arteni massif [1], and the other is from an impactite [2]. No report about the existence of oldhamite in the mantle. However, oldhamite resulted from the condensation of the nebula gas is potentially abundant on Mercury's surface (Fig. 1) [3], which is closest to the Sun among the 8 planets in the solar system, and it is a common mineral in enstatite chondrites [4], which was considered to be formed near the center of the solar nebula within the orbit of Mercury (Fig. 1) [5]. In both cases, the highly reducing conditions with an oxygen fugacity well below IW-2.7 (IW = iron-wüstite redox buffer, in  $\lg f\text{O}_2$ ) stabilize oldhamite [6]. It seems that the initial formation of oldhamite was in the region close to the Sun, at Mercury's surface, or within the orbit of Mercury (Fig. 1). At present, there is no discussion about the origin of oldhamite in Earth, and previous

studies focused on the origin of this mineral in enstatite chondrites. There are currently [two views](#) regarding this issue.

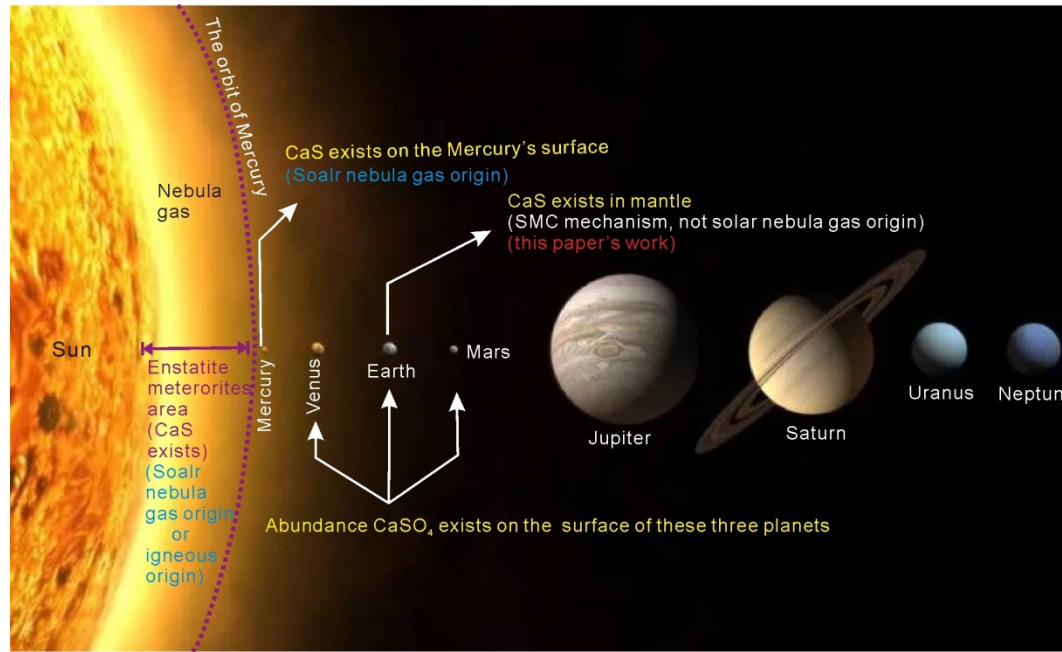


**Fig. 1.** The main distribution of oldhamite (CaS) and anhydrite (CaSO<sub>4</sub>) in the Solar System.

Most scholars held the view that oldhamite in enstatite chondrites is a product of condensation of the solar nebula gas (Fig. 1). Laboratory smoke experiments demonstrate that pure CaS condense from vapor phases of calcium and sulfur [7]. This supports a nebular gas origin and, according to first-principles calculations at equilibrium, oldhamite is more easily enriched in light Ca isotopes than other solid minerals. In contrast, condensed Ca-bearing minerals from nebular gas are enriched in heavy Ca isotopes relative to the residual gaseous Ca [8]. Oldhamite in enstatite chondrites is isotopically heavier than coexisting silicate materials, supporting the solar nebular gas origin. However, sulfur isotope data do not support the solar nebula gas

origin. The correlation between  $\Delta^{33}\text{S}$  and  $\Delta^{36}\text{S}$  of some enstatite chondrites does not follow the trends of photochemistry in the solar nebula with  $\Delta^{36}\text{S} = -2.98\Delta^{33}\text{S}$  [9] and of cosmic-ray spallation with  $\Delta^{36}\text{S} = 8\Delta^{33}\text{S}$  [10].

Some scholars argue that the oldhamite in enstatite chondrites is of igneous origin rather than the solar nebula gas origin [11]. Textural evidence includes apparent primary igneous grain boundaries between oldhamite and forsterite and the presence of round, droplet-like Mn-Fe-Mg-Cr-Na sulfide inclusions within oldhamite, which appear to represent an immiscible sulfide liquid [11].

Our experimental petrology work in this study shows that oldhamite can exist in the mantle. This work provides a quite different genetic model for oldhamite and expands the position where oldhamite can exist in the solar system (Fig. 1). Furthermore, we prove that whether a large amount of CaS or CaSO<sub>4</sub> appears on the surface of a planet is closely related to the oxygen fugacity of the planetary magma and atmospheric composition. This paper could shed light on the formation of alkaline-earth metal sulfides, the origin of enstatite chondrites, C-O-S-Ca cycles, the mantle metasomatism mechanism, the crustal contamination process of mantle-derived magma, and planetary habitability.

## Results

### *High P-T experiments*

Here we show that oldhamite forms under conditions compatible with the Earth's upper mantle through the reaction between sulfide-bearing orthopyroxenite and  $\text{CaCO}_3$  at 1.5 GPa/1510 K and 0.5 GPa/1320 K in a graphite-lined  $\text{Au}_{75}\text{Pd}_{25}$  capsule (Fig. 2). Oldhamite was observed in the central reaction zone of recovered samples (Figs. 2 and S4). Hereafter we refer to this formation process as the sulfide-magma-calcite (SMC) interaction. In the absence of  $\text{CaCO}_3$ , experiments under otherwise identical conditions produce partial melt from orthopyroxenite are similar in composition. In both cases, the melts are high-Mg basaltic magmas (with  $\text{SiO}_2 = 54.5\text{--}54.9$  wt%,  $\text{MgO} = 9.54\text{--}10.19$  wt%; Supplementary Section 4 and Table S3).

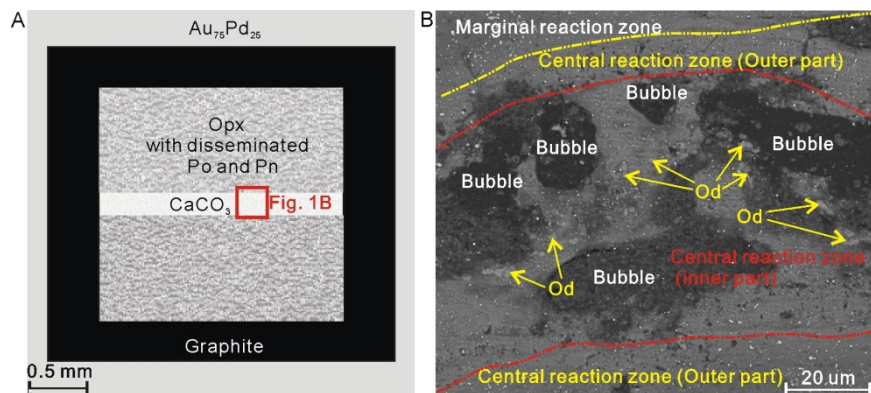
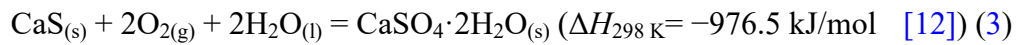
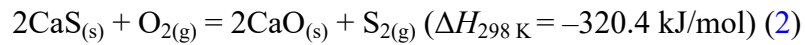


**Fig. 2.** State and location of CaS generated by the interaction of sulfide-bearing magma-calcite (SMC). (A) Reaction chamber for the contamination experiments between the Po-Pn-bearing orthopyroxenite and  $\text{CaCO}_3$ ; (B) Drop-shaped CaS in the inner part of the central reaction zone and disseminated Fe-Ni sulfide (bright white). Abbreviations: Opx = orthopyroxenite, Po = pyrrhotite, Pn = pentlandite, and Od = oldhamite.

## **Determination of oxygen fugacity environment for the stable existence of oldhamite**

In natural terrestrial samples, the occurrence of CaS is generally constrained by the following reactions



As seen from these equations, CaS can be easily oxidized to form  $\text{CaSO}_4$  or  $\text{CaSO}_4 \cdot 2\text{H}_2\text{O}$ . Thus, the stable existence of CaS depends mainly on the oxygen fugacity. In order to quantitatively calculate the oxygen fugacity boundary where CaS can exist stably, this paper defines two oxygen buffers in the world for the first time: **OA buffer** and **OLS buffer**. The oxygen fugacity at the oldhamite-anhydrite equilibrium (Equation 1, named the **OA buffer**) and the oldhamite-lime-sulfur equilibrium (Equation 2, named the **OLS buffer**) can be determined by Equations 4 and 5, respectively.

$$\lg f_{\text{O}_2} = 2.19144 + 1.09305 \times 10^{-4} T - 25137/T - 1551.42/T^2 + 1.5305 \times 10^7/T^3 + 0.04777P/T + 2.7838\lg T \quad (4)$$

$$\lg f_{\text{O}_2} = -21.1162 + 3.65342 \times 10^7/T^3 - 6205.07/T^2 + (-16237.94 - 0.11450P)/T + 0.43722 \times 10^{-3}T + 11.13544\lg T + \lg f_{\text{S}_2} \quad (5)$$

where  $P$  is pressure in bar, and  $T$  is temperature in K. The detail process for the quantitative formula calculation of these two buffers is listed in the **Supplementary**

[Section 5](#). The  $T$ -  $\lg f_{\text{O}_2}$  curves of these two buffers are shown in [Fig. 3](#). At 0.5 GPa and 1320 K,  $\text{OA} = \text{FMQ} + 2.21 = \text{IW} + 6.05$  ( $\lg f_{\text{O}_2} = -7.83$ ) and  $\text{OLS} = \text{FMQ} - 0.52 = \text{IW} + 3.30$  ( $\lg f_{\text{O}_2} = -10.57$ ) ([Fig. 3](#)). If the oxygen fugacity value is lower than  $\text{OLS}$ , oldhamite is stable. On the contrary, the oxygen fugacity value of the anhydrite stable field is higher than  $\text{OA}$ .

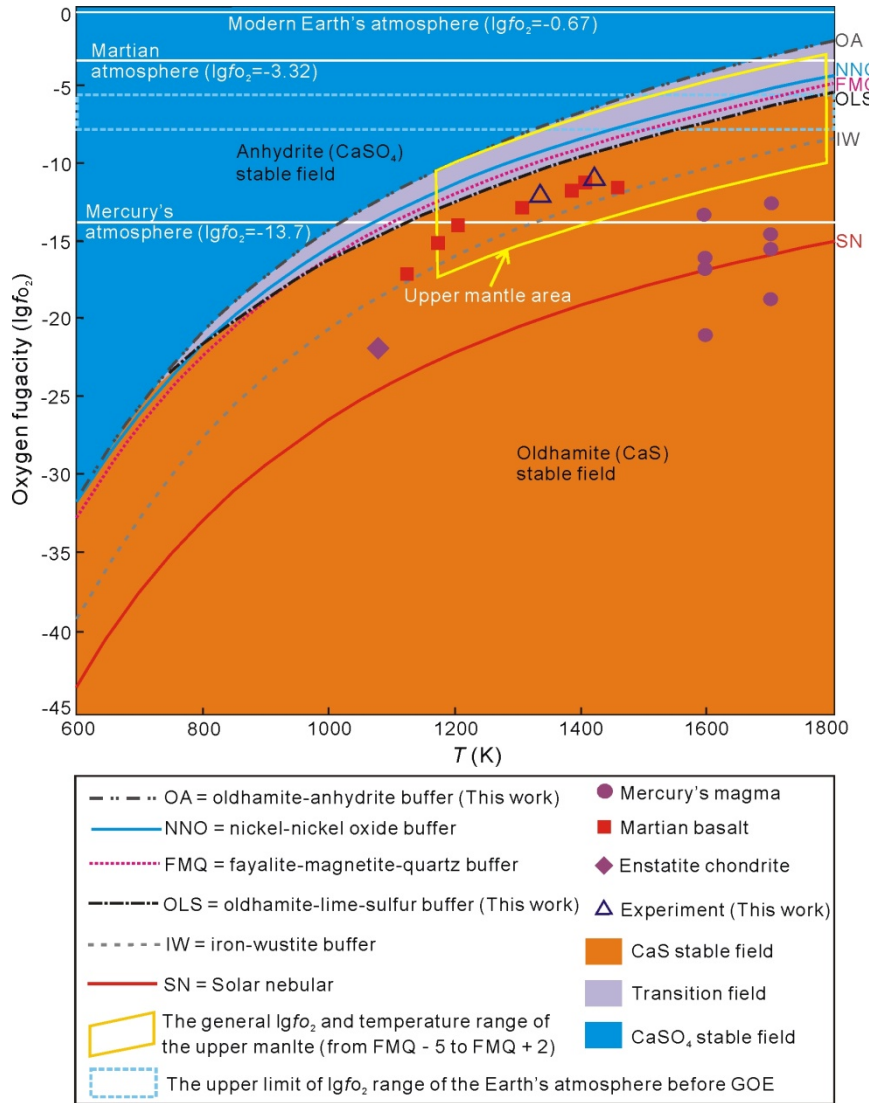


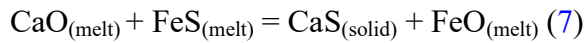
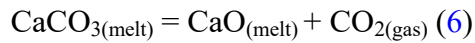
**Fig. 3. Representative oxygen fugacity buffer at 0.5 GPa total pressure vs. temperature curves and the distributions of some natural and experimental samples.** References: NNO is from Ref. [13], and FMQ and IW are from Ref. [14];  $\lg f_{\text{S}_2}$  value of  $-12$  (mean sulfur fugacity of black smoker [15]) was used during the

OLS calculation. Values of solar nebula  $\lg f_{\text{O}_2}$  are calculated from the equation  $\lg f_{\text{O}_2} = -0.85 - 25,664/T$ , where  $T$  is in K [16]. The  $\lg f_{\text{O}_2}$  values of enstatite chondrite, Martian basalt, and the silicate melts on Mercury's surface are from Ref. [6], Ref. [17], and Ref. [18], respectively. The general  $\lg f_{\text{O}_2}$  and temperature range of the upper mantle is from Ref. [19] and Ref. [20], respectively. The upper limit of  $\lg f_{\text{O}_2}$  range of the Earth's atmosphere is from Ref. [21].

## Discussion

### *New formation mechanism of oldhamite*

The partial melts from orthopyroxenite in our experiments are high-Mg basaltic melts. This is consistent with the partial melting process of mantle pyroxenites that in part produced mid-ocean ridge basalts (MORBs) and Hawaiian shield basalts [22, 23]. It is worth noting that similar high-Mg basaltic melt is the parent magma of some magmatic Cu-Ni-Pt deposits in orogenic belts or related to mantle plume [24]. These melts are derived from the mantle but usually interacted with crustal carbonate. The oxygen fugacity in the graphite-lined noble metal capsule used in this study is about FMQ-2.1 [25] (FMQ = fayalite-magnetite-quartz redox buffer, in  $\lg f_{\text{O}_2}$ ). Hence, our experiments simulate the reaction between basaltic and carbonate magma in the mantle, the metasomatism of the mantle by carbonate melts, and the reaction process between basaltic magma and crustal carbonate. Based on our findings (Fig. 2), oldhamite can exist in the mantle under these conditions. In our run products, pentlandite or pyrrhotite is present around oldhamite, and cavities formed by bubbles are always present close to oldhamite (Figs. 2 and S4). Hence, the most probable route for CaS formation is:



Here, we name this process as the SMC model (sulfide-magma-calcite interaction model).

The SMC model is different from the previous genetic model **in three ways**. **The first difference** is about the formation location. Previous researches believed that oldhamite exists in the enstatite meteorite or on the surface of Mercury [3, 4], but this study proved that it could be stable in the mantle. We can speculate that it could be formed in the interior of other terrestrial planets with magmatic activities. **The second difference** is that the formation process by the sulfide-magma-calcite interaction in this study is totally different from the nebula gas mechanism. **The third difference** is about the oxygen fugacity. Former research thought that an oxygen fugacity below IW-2.7 (IW = iron-wüstite redox buffer, in  $\text{lgf}_{\text{O}_2}$ ) is necessary for the stable existence of oldhamite in the solar nebula model [6]. However, our experiment and calculation results show that the oldhamite can be stable below IW + 3.3 (Fig. 3), which is 6 orders of magnitude higher than the solar nebula mechanism. This greatly expands the oxygen fugacity range where oldhamite can exist stably.

### ***The preservation conditions of oldhamite on the surface of a planet***

The oldhamite can exist in mantle, but why it hardly to be found on the Earth's surface? A closer look at the redox conditions of the **hosting magma** and **atmosphere** is required. Oldhamite is stable when  $\text{lgf}_{\text{O}_2}$  is below the OLS buffer, but

cannot exist when  $\lg f_{O_2}$  is above the OA buffer (Fig. 3). The  $\lg f_{O_2}$  values of Mercury's surface magma range from IW-2.93 to -10.5 ( $\lg f_{O_2} = -13.2$  to -21.7) at 1600–1700 K (Fig. 3), and the  $\lg f_{O_2}$  value of Mercury's atmosphere is -14.7. These values are much below the OLS buffer (Fig. 3), permitting the conservation of oldhamite. That is, the widespread presence of oldhamite on the surface of a planet indicates an extremely anoxic environment. On the other side, as the  $\lg f_{O_2}$  value of -4.32 of the Martian atmosphere is higher than OLS, no oldhamite but some sulfates have been found on Mars, despite the  $\lg f_{O_2}$  of Martian magma is lower than OLS (Fig. 3). It means that the extreme low oxygen content in the atmosphere is necessary for the preservation of oldhamite, which is unsuitable for most known organisms to survive. Interestingly, Earth takes an intermediate position between these two cases (though closer to Mars). The average  $\lg f_{O_2}$  values for arc basalts (FMQ + 0.96), ocean island magma (FMQ + 0.82), and most basalt related to mantle plumes on Earth (FMQ + 0.1) are higher than OLS [26]. Moreover, the  $\lg f_{O_2}$  value of -0.67 of Earth's atmosphere is much higher than OA (Fig. 3). The habitable surface conditions for human on Earth do not support the preservation of oldhamite.

### ***The possible link between oldhamite and anhydrite in black smokers***

Most of the oxygen fugacities of the upper mantle are located in the oldhamite stable field (Fig. 3), but it hardly to be found on the Earth's surface. A reasonable explanation is the existence of an interface where  $\text{CaS}$  is converted to  $\text{CaSO}_4$  between the upper mantle and the surface. On Earth, the MORBs are characterized by a redox

state of  $\text{FMQ}-0.41\pm0.43$  (Fig. S5) [27], which are closed to  $\text{FMQ}-0.52$ , the upper limit oxygen fugacity for the stable existence of oldhamite (Fig. 3). There is a large amount of anhydrite and gypsum in the mid-ocean ridges black smoker system. Thus, the interface where  $\text{CaS}$  is converted to  $\text{CaSO}_4$  may exist near or at the solidified MORBs (Fig. S5). In the mantle underneath mid-ocean ridges, the conditions for the formation of  $\text{CaS}$  including carbonate magma and sulfide-bearing magma sometimes can be met. At a depth of about 160–170 km, diamond is expected to convert into graphite at an oxygen fugacity above  $\text{FMQ}-2$  (Fig. S5) [28, 29]. Redox melting [ $\text{C}(\text{graphite}) + 2\text{Fe}_2\text{O}_3(\text{melt}) + \text{O}^{2-}(\text{melt}) = 4\text{FeO} + \text{CO}_3^{2-}$  (both in the melt)] is believed to take place at a depth of around 120–150 km with an oxygen fugacity about  $\text{FMQ}-1.6$  (Fig. S5) [29]. The carbonate melt produced by the redox melting will ascend as a flux into the overlying mantle [30]. The interaction between carbonate melt and sulfide-bearing magma could happen.

The  $\delta^{34}\text{S}_{\text{V-CDT}}$  value of anhydrite in the mid-ocean ridges black smoker system gradually decreases from the seawater's value of  $20\pm1$  to  $3.4\text{\textperthousand}$ , as observed in the 1.8 km deep drillhole in a middle-ocean ridge [31]. The  $\delta^{34}\text{S}_{\text{V-CDT}}$  value of  $3.4\text{\textperthousand}$ , which is much lower than that of modern seawater, is considered to have resulted from the oxidation of low- $\delta^{34}\text{S}$  sulfide to sulfate in the MORB [32]. Oldhamite is easily oxidized due to the large negative  $\Delta H_{298\text{K}}$  value for Equation 1. Thus, the oxidation of  $\text{CaS}$  to  $\text{CaSO}_4$  could be a viable route for the formation of sulfate. At 1543 K, the melt temperature of MORB, the sulfur and calcium isotopic fractionation between anhydrite (Anh) and oldhamite (Od) are  $\delta^{34}\text{S}_{\text{V-CDT}}^{\text{Anh}} - \delta^{34}\text{S}_{\text{V-CDT}}^{\text{Od}} = 10.21\text{\textperthousand}$  and

$\delta^{44/40}\text{Ca}^{\text{Anh}} - \delta^{44/40}\text{Ca}^{\text{Od}} = 0.18\text{\textperthousand}$ , respectively (The detail calculation process please see Section 6 in the Supplementary). On the contrary, at the same temperature, the sulfur fractionation between sulfate and pyrite, the most abundant sulfide in MORB, is  $\delta^{34}\text{S}_{\text{V-CDT}}^{\text{Sulfate}} - \delta^{34}\text{S}_{\text{V-CDT}}^{\text{Pyrite}} = 3.19\text{\textperthousand}$  [33]. However, the lowest reported sulfur isotope of anhydrite is 3.4‰, which is 5.2 ‰ higher than the mantle sulfur isotope (i.e.,  $\delta^{34}\text{S}_{\text{V-CDT}} = -1.80\text{\textperthousand}$  [34]). Such high isotopic fractionation is difficult to be achieved with only fractionation between sulfate and pyrite. It calls for the role of oldhamite due to relatively large sulfur isotopic fractionation between  $\text{CaSO}_4$  and  $\text{CaS}$ .

**On the other hand**, oldhamite is more easily enriched in light Ca isotopes than the other Ca-bearing minerals [8, 35]. The dissolution of  $\text{CaSO}_4$  that have experienced the  $\text{CaS-CaSO}_4$  isotopic fractionation into hydrothermal fluids at the mid-ocean ridges is expected to increase the  $\delta^{44/40}\text{Ca}$  value of hydrothermal fluids relative to the host-rocks, which, indeed, is observed [36]. Thus, the oxidation of  $\text{CaS}$  offers a viable alternative for the origin of anhydrite in the mid-ocean ridges black smoker system.

We do not deny that the formation mechanism of most gypsum in the mid ocean ridge is due to the solubility of Ca and  $\text{SO}_4^{2-}$  in seawater decreases with the increase of temperature [37, 38]. The new sulfate formation mechanism:  $\text{CaS}$  oxidation model in this paper, can explain some special Ca-S isotope characteristics, which is an supplement to the formation process of sulfate on planets.

### ***The Influence of oldhamite in Earth on atmospheric composition***

The Earth's deep interior holds the key to habitability [39-43]. In this chapter, we

discuss two events that oldhamite may affect the atmospheric composition. The first is why the Earth's atmosphere before the Great Oxidation Event (GOE) was anoxic or oxygen free. Many evidence show that Earth's atmosphere was initially free of O<sub>2</sub> [44, 45]. Around 2.46 to 1.85 billion years ago (Ga), oxygen levels rose from  $<10^{-7.1} - 10^{-5.1}$  that of present atmospheric levels (PAL) ( $\lg f_{O_2} < -7.6$  to  $-6.0$ , Fig. 3) to  $10^{-4.6} - 10^{-2.0}$  PAL ( $\lg f_{O_2} = -5.3$  to  $-2.7$ ) [21], known as the GOE. To explore the reasons for the anoxic or oxygen free feature of the early Earth's atmosphere, we need to clarify the characteristics of the initial materials that were used to build the Earth. Enstatite chondrite, one of the most important repositories of oldhamite, have similar isotopic composition to terrestrial rocks, so are often considered to be the representative of the material which formed Earth [46, 47]. That is, the early Earth contains enough oldhamite. The upper limit of  $\lg f_{O_2}$  range of the Earth's atmosphere before GOE is from  $-7.6$  to  $-6.0$  (Fig. 3) [21], which partially overlaps with the oldhamite stable field. Moreover, the oxidation of oldhamite to CaSO<sub>4</sub> means the consumption of oxygen (Equation 1). We can speculate that the existence of oldhamite perhaps contributed to the maintenance of anoxic or oxygen free environment before GOE. After GOE, the  $\lg f_{O_2}$  of the Earth's atmosphere at about 1.85 Ga ranges from  $-5.3$  to  $-2.7$  [21], which is higher than OLS. According to the above logic, some CaSO<sub>4</sub> would appear on Earth after GOE. The geological facts are exactly as we expected. Calcium sulfate (CaSO<sub>4</sub>) occurred in the 2.2 Ga sedimentary rocks in the Yerrida rift basin of Western Australia [48]. Thus, oldhamite perhaps played a role for the anoxic or oxygen free Earth's atmosphere before GOE.

**The second** event that oldhamite may have an effect on the atmospheric composition was the Permian–Triassic Boundary (PTB) mass extinction. The formation of 1 mole of CaS is accompanied by the production of 1 mole of CO<sub>2</sub> (Equations 6-7); during the oxidation of CaS to sulfate, the oxidation of 1 mole CaS will lead to the consumption of 2 moles O<sub>2</sub> (Equation 1). During the PTB mass extinction, it shows a sharp increase of atmospheric CO<sub>2</sub> and a decrease of atmospheric O<sub>2</sub> content. The atmospheric CO<sub>2</sub> concentration at the PTB is estimated to have been (3314 ± 1097) ppm, which is more than double the Permian average and is (12 ± 4) times that of the current atmosphere [49]. The atmospheric oxygen underwent a very sharp drop from 30 to 15% (volume fraction) at the PTB [50]. The reaction between mantle magma and crustal rocks in Siberian large igneous province (SLIP) is believed to be an important trigger for the above atmospheric composition change [51-53]. The SLIP is characterized by low magnesium tholeiitic basalts with MgO < 7 wt% [54]. This composition is approximately similar to the composition of the initial melt formed by the partial melting of orthopyroxenite in this study (Table S3). The magma of SLIP is characterized by a low oxygen fugacity with a value of FMQ-1.5 [54]. Moreover, some famous magmatic Cu-Ni-PGE sulfide deposits formed at the SLIP, indicating some sulfide-rich magma existed. The above features met the conditions for the formation of CaS. Thus, the intermediate effect of CaS, accompanied by CO<sub>2</sub> generation and O<sub>2</sub> consumption, is hardly be excluded during the interaction process between the upwelling of large-scale S-bearing reducing magma from mantle and the crustal carbonate rocks in the SLIP.

## Conclusions

Two geological processes are likely to involve oldhamite as a transient phase, including mantle metasomatism process by carbonate melts beneath the MORB region and crustal contamination process of mantle derived magma during the formation of some magmatic Cu-Ni-PGE sulfide deposits at large igneous province. Oldhamite is a plausible precursor for igneous Ca-sulfate in MORB. The formation and oxidation of oldhamite are accompanied by the production of CO<sub>2</sub> and the consumption of O<sub>2</sub>, which have more or less influence on the atmospheric composition. The widespread existence of oldhamite on the planet's surface indicates that the magma of the planet has low oxygen fugacity and extreme low oxygen content in atmosphere, which is not habitable. Human are lucky because natural oldhamite on the Earth's surface is extremely rare.

## Methods

### *High P-T experiments*

Experimental petrological methods are used to simulate the formation process of oldhamite in the mantle. The initial material is pyrrhotite-pentlandite-bearing orthopyroxenite and CaCO<sub>3</sub> powder. The mineral composition and chemical composition of starting materials were described in the [Supplementary section 1](#). Experiments were conducted at 0.5 GPa/1320 K and 1.5 GPa/1510 K, using a 2000-tons multi-anvil cubic apparatus at the University of Nevada, Las Vegas.

Sample powder was packed in a graphite crucible placed in an Au<sub>75</sub>Pd<sub>25</sub> outer capsule with outer diameter of 3 mm ([Fig. S3a](#)). The mineral and melt composition analysis after the experiment is completed by electron microprobe. Please refer to [Supplementary section 3](#) for the parameter design of the electron probe.

### ***The determination of oxygen fugacity***

The oxygen fugacities at the oldhamite-lime-sulfur equilibrium (OLS buffer) and at oldhamite-anhydrite equilibrium (OA buffer) were obtained by thermodynamic calculation. The detail calculation processes were listed in the [Supplementary section 5](#).

The concept of oxygen fugacity of rocks has been deeply rooted in people's minds, but some researchers are not familiar with the oxygen fugacity of atmosphere. Here, we explain the calculation process of oxygen fugacity of modern Earth's atmosphere. Oxygen accounts for 21% of the modern Earth's atmospheric volume, so the partial pressure of oxygen is 0.21 bars. Then,  $\log (0.21) = -0.67$ . This is, the  $\lg f_{O_2}$  of modern Earth's atmosphere is  $-0.67$  ([Fig. 3](#)). Similarly, the oxygen fugacities of the Mercury 's atmosphere and Martian atmosphere are also calculated in [Supplementary section 5.1](#).

### ***The determination of isotope fractionation***

The Sulfur isotope fractionation between CaS and CaSO<sub>4</sub> was calculate by the method of

Ref. [55] combined with the infrared and Raman frequencies of oldhamite and anhydrite. For more detail, please see the [Supplementary section 6.1](#).

Former researchers have calculated the polynomial fitting of the ratio of reduced partition function for  $^{44}\text{Ca}/^{40}\text{Ca}$  of oldhamite and anhydrite by the static first-principles calculation [8, 35]. Based on these results, the equilibrium Ca isotope fractionation between  $\text{CaSO}_4$  and  $\text{CaS}$  was inferred. The inferred equation was listed in the [Supplementary section 6.2](#).

## Acknowledgments

We are very grateful to Professor D.L. Khoslstedt from the University of Minnesota-Twin City and Professor Y.G. Xu and Dr. Z.Y. Luo from the Guangzhou Institute of Geochemistry, Chinese Academy of Sciences for their assistance in experimental petrology and sample preparation. Professor F. Huang and C. Zhou from the University of Science and Technology of China are acknowledged for their great help in S-Ca isotope fractionation calculation.

This work was supported by the Hainan Provincial Joint Project of Sanya Yazhou Bay Science and Technology City (2021CXLH0027 to Y.G.L.), the Chinese Academy of Sciences (QYZDY-SSW-DQC008 to I.M.C, and QYZDY-SSW-DQC029 and XDA22040501 to S.H.M.), and Municipal Development and Reform Commission of Shenzhen (L.P.W.)

### Author contributions:

Conceptualization: Y.G.L., I.M.C., S.H.M.

Methodology: Y.G.L., J.Z.C., L.P.W., O.T., N.P.W., W.Y.L., and M.H.R.

Investigation: S.B.B., D.L.A., M.P.W., and L.O.

Visualization: Y.G.L., I.M.C., J.Z.C., W.Y.L., and M.H.R.

Supervision: L.P.W., S.H.M., I.M.C.

Writing—original draft: Y.G.L., J.Z.C., I.M.C., and O.T.

Writing—review & editing: S.H.M., L.P.W., L.O., and M.H.R.

**Competing interests:** Authors declare that they have no competing interests.

**Data and materials availability:** All data are available in the main text or the supplementary materials.

## References

1. Nasedkin V and Boyarskaya R. Minerals in volcanic-glass pores. *Int Geol Rev* 1982; **24**: 1101-1108.
2. Yanev Y, Benderev A and Zotov N, *et al.* Exotic rock block from the Koshava gypsum mine, Northwest Bulgaria: Petrography, geochemistry, mineralogy and melting phenomena. *Geol Balk* 2021; **50**: 45-65.
3. Bennett C J, McLain J L and Sarantos M, *et al.* Investigating potential sources of Mercury's exospheric Calcium: Photon-stimulated desorption of Calcium Sulfide. *J Geophys Res: Planets* 2016; **121**: 137-146.
4. Defouilloy C, Cartigny P and Assayag N, *et al.* High-precision sulfur isotope composition of enstatite meteorites and implications of the formation and evolution of their parent bodies. *Geochim Cosmochim Acta* 2016; **172**: 393-409.
5. Kallenbach R, Encrenaz T and Geiss J, *et al.* Solar System History from Isotopic Signatures of Volatile Elements. in Kallenbach R (ed.). *Solar System History from Isotopic Signatures of Volatile Elements*: Springer Science & Business Media, 2012, 413-422.
6. Brett R and Sato M. Intrinsic oxygen fugacity measurements on seven chondrites, a pallasite, and a tektite and the redox state of meteorite parent bodies. *Geochim Cosmochim Acta* 1984; **48**: 111-120.
7. Yokoyama K, Kimura Y and Kaito C. Experiments on condensation of calcium sulfide grains to demarcate environments for the formation of enstatite chondrites. *ACS Earth Space Chem* 2017; **1**: 601-607.
8. Huang F, Zhou C and Wang W, *et al.* First-principles calculations of equilibrium Ca isotope fractionation: Implications for oldhamite formation and evolution of lunar magma ocean. *Earth Planet Sci Lett* 2019; **510**: 153-160.
9. Chakraborty S, Jackson T L and Ahmed M, *et al.* Sulfur isotopic fractionation in vacuum UV photodissociation of hydrogen sulfide and its potential relevance to meteorite analysis. *Proc Natl Acad Sci USA* 2013; **110**: 17650-17655.
10. Farquhar J, Jackson T L and Thiemens M H. A  $^{33}\text{S}$  enrichment in ureilite meteorites: evidence for a nebular sulfur component. *Geochim Cosmochim Acta* 2000; **64**: 1819-1825.

11. Wheelock M M, Keil K and Floss C, *et al.* REE geochemistry of oldhamite-dominated clasts from the Norton County aubrite: Igneous origin of oldhamite. *Geochim Cosmochim Acta* 1994; **58**: 449-458.
12. Robie R A and Hemingway B S. Thermodynamic properties of minerals and related substances at 298.15 K and 1 bar ( $10^5$  Pascals) pressure and at higher temperatures. U.S. Geological Survey Bulletin ed. 1995: US Government Printing Office.
13. O'neill H S. Free energies of formation of NiO, CoO,  $\text{Ni}_2\text{SiO}_4$ , and  $\text{Co}_2\text{SiO}_4$ . *Am Mineral* 1987; **72**: 280-291.
14. O'neill H S. Quartz-fayalite-iron and quartz-fayalite-magnetite equilibria and the free energy of formation of fayalite ( $\text{Fe}_2\text{SiO}_4$ ) and magnetite ( $\text{Fe}_3\text{O}_4$ ). *Am Mineral* 1987; **72**: 67-75.
15. Keith M, Haase K M, Schwarz-Schampera U, *et al.* Effects of temperature, sulfur, and oxygen fugacity on the composition of sphalerite from submarine hydrothermal vents. *Geology* 2014; **42**: 699-702.
16. Krot A N, Fegley Jr B and Lodders K, *et al.* Meteoritical and astrophysical constraints on the oxidation state of the solar nebula. *Protostars Planets IV* 2000; **1019**.
17. Herd C D, Borg L E and Jones J H, *et al.* Oxygen fugacity and geochemical variations in the Martian basalts: Implications for Martian basalt petrogenesis and the oxidation state of the upper mantle of Mars. *Geochim Cosmochim Acta* 2002; **66**: 2025-2036.
18. Zolotov M Y, Sprague A L and Hauck S A, *et al.* The redox state, FeO content, and origin of sulfur-rich magmas on Mercury. *J Geophys Res: Planets* 2013; **118**: 138-146.
19. Frost D J and Mccammon C A. The redox state of Earth's mantle. *Annu Rev Earth Planet Sci* 2008; **36**: 389-420.
20. Faul U H and Jackson I. The seismological signature of temperature and grain size variations in the upper mantle. *Earth Planet Sci Lett* 2005; **234**: 119-134.
21. Kanzaki Y and Murakami T. Estimates of atmospheric  $\text{O}_2$  in the Paleoproterozoic from paleosols. *Geochim Cosmochim Acta* 2016; **174**: 263-290.
22. Sobolev A V, Hofmann A W, Sobolev S V, *et al.* An olivine-free mantle source of Hawaiian shield basalts. *Nature* 2005; **434**: 590.
23. Lambert S, Laporte D and Schiano P. An experimental study of pyroxenite partial melts at 1 and 1.5 GPa: Implications for the major-element composition of Mid-Ocean Ridge Basalts. *Earth Planet Sci Lett* 2009; **288**: 335-347.

24. Li C and Ripley E M. The giant Jinchuan Ni-Cu-(PGE) deposit; tectonic setting, magma evolution, ore genesis, and exploration implications. *Rev Econ Geol* 2011; **17**: 163-180.
25. Li Y and Audétat A. Partitioning of V, Mn, Co, Ni, Cu, Zn, As, Mo, Ag, Sn, Sb, W, Au, Pb, and Bi between sulfide phases and hydrous basanite melt at upper mantle conditions. *Earth Planet Sci Lett* 2012; **355**: 327-340.
26. Cottrell E, Birner S K and Bounce M, *et al*. Oxygen fugacity across tectonic settings. in Moretti R and Neuville D (ed.). *Magma Redox Geochemistry*: Wiley, 2021, 33-61.
27. Bézos A and Humler E. The  $\text{Fe}^{3+}/\Sigma\text{Fe}$  ratios of MORB glasses and their implications for mantle melting. *Geochim Cosmochim Acta* 2005; **69**: 711-725.
28. Stagno V and Frost D J. Carbon speciation in the asthenosphere: Experimental measurements of the redox conditions at which carbonate-bearing melts coexist with graphite or diamond in peridotite assemblages. *Earth Planet Sci Lett* 2010; **300**: 72-84.
29. Stagno V, Ojwang D O and Mccammon C A, *et al*. The oxidation state of the mantle and the extraction of carbon from Earth's interior. *Nature* 2013; **493**: 84-88.
30. Dasgupta R and Hirschmann M M. The deep carbon cycle and melting in Earth's interior. *Earth Planet Sci Lett* 2010; **298**: 1-13.
31. Teagle D A, Alt J C and Halliday A N. Tracing the chemical evolution of fluids during hydrothermal recharge: Constraints from anhydrite recovered in ODP Hole 504B. *Earth Planet Sci Lett* 1998; **155**: 167-182.
32. Alt J C, Zuleger E and Erzinger J. Mineralogy and stable isotopic compositions of the hydrothermally altered lower sheeted dike complex, Hole 504B, Leg 140. in *Proceedings of the Ocean Drilling Program, Scientific Results*: Citeseer, 1995, 155-166.
33. Ohmoto H. Isotopes of sulfur and carbon. in *Geochemistry of hydrothermal ore deposits*: John Wiley & Sons, 1979, 509-567.
34. Labidi J, Cartigny P and Moreira M. Non-chondritic sulphur isotope composition of the terrestrial mantle. *Nature* 2013; **501**: 208-211.
35. Zhou C. Theoretical calculations of the equilibrium Ca isotope fractionation factors. *Master. Thesis*. University of Science and Technology of China, 2019.
36. Amini M, Eisenhauer A and Böhm F, *et al*. Calcium isotope ( $\delta^{44/40}\text{Ca}$ ) fractionation along hydrothermal pathways, Logatchev field (Mid-Atlantic Ridge,  $14^{\circ}45'N$ ). *Geochim Cosmochim Acta* 2008; **72**: 4107-4122.
37. Bischoff J L and Seyfried W E. Hydrothermal chemistry of seawater from 25 degrees to 350 degrees C. *Am J Sci* 1978; **278**: 838-860.

38. Newton R C and Manning C E. Solubility of anhydrite, CaSO<sub>4</sub>, in NaCl–H<sub>2</sub>O solutions at high pressures and temperatures: applications to fluid–rock interaction. *J Petrol* 2005; **46**: 701-716.
39. Mao H K, Hu Q and Yang L et al. When water meets iron at Earth's core–mantle boundary. *Natl Sci Rev* 2017; **4**: 870–8.
40. Zhang L, Zhang L and Tang M, *et al.* Massive abiotic methane production in eclogite during cold subduction. *Natl Sci Rev* 2022. <https://doi.org/10.1093/nsr/nwac207>
41. Liu J and Mao H K. Yi-Gang Xu: the Earth's deep interior holds the key to habitability. *Natl Sci Rev* 2021; **8**: nwab018.
42. Zhu R, Hou Z and Guo Z, *et al.* Summary of “the past, present and future of the habitable earth: Development strategy of earth science”. *Chin Sci Bull* 2021; **66**: 4485-4490.
43. Hu Q, Kim D Y and Yang W, *et al.* FeO<sub>2</sub> and FeOOH under deep lower-mantle conditions and Earth's oxygen–hydrogen cycles. *Nature* 2016; **534**: 241-244.
44. Lee C T, Yeung L Y and Mckenzie N R, *et al.* Two-step rise of atmospheric oxygen linked to the growth of continents. *Nat Geosci* 2016; **9**: 417-424.
45. Lyons T W, Reinhard C T and Planavsky N J. The rise of oxygen in Earth's early ocean and atmosphere. *Nature* 2014; **506**: 307-315.
46. Piani L, Marrocchi Y and Rigaudier T, *et al.* Earth's water may have been inherited from material similar to enstatite chondrite meteorites. *Science* 2020; **369**: 1110-1113.
47. Javoy M, Kaminski E and Guyot F, *et al.* The chemical composition of the Earth: Enstatite chondrite models. *Earth Planet Sci Lett* 2010; **293**: 259-268.
48. El Tabakh M, Grey K and Pirajno F, *et al.* Pseudomorphs after evaporitic minerals interbedded with 2.2 Ga stromatolites of the Yerrida basin, Western Australia: origin and significance. *Geology* 1999; **27**: 871-874.
49. Retallack G J. A 300-million-year record of atmospheric carbon dioxide from fossil plant cuticles. *Nature* 2001; **411**: 287-290.
50. Berner R A. GEOCARBSULF: a combined model for Phanerozoic atmospheric O<sub>2</sub> and CO<sub>2</sub>. *Geochim Cosmochim Acta* 2006; **70**: 5653-5664.
51. Sobolev S V, Sobolev A V and Kuzmin D V, *et al.* Linking mantle plumes, large igneous provinces and environmental catastrophes. *Nature* 2011; **477**: 312-316.
52. Li M, Grasby S E and Wang S-J, *et al.* Nickel isotopes link Siberian Traps aerosol particles to the end-Permian mass extinction. *Nat Commun* 2021; **12**: 1-7.
53. Yin H, Jiang H and Xia W, *et al.* The end-Permian regression in South China and its implication on mass extinction. *Earth-Sci Rev* 2014; **137**: 19-33.

54. Sobolev A V, Krivolutskaya N A and Kuzmin D. Petrology of the parental melts and mantle sources of Siberian trap magmatism. *Petrology* 2009; **17**: 253-286.
55. Bigeleisen J and Mayer M G. Calculation of equilibrium constants for isotopic exchange reactions. *J Chem Phys* 1947; **15**: 261-267.